Journal of Nuclear Materials 403 (2010) 108–112

Contents lists available at ScienceDirect

Journal of Nuclear Materials

journal homepage: www.elsevier.com/locate/jnucmat

Ion-induced damage in graphite: A Raman study

A. Theodosiou, A.F. Carley *, S.H. Taylor

Cardiff University, Chemistry Department, Main Building, Park Place, Cardiff CF10 3AT, United Kingdom

ARTICLE INFO

Article history:
Received 21 January 2010
Accepted 3 June 2010

ABSTRACT

A Raman investigation has been carried out on samples of ion irradiated highly-oriented pyrolytic graphite (HOPG). Irradiation is carried out under ultra-high vacuum (UHV), at room temperature, with 5 keV He^+, Ne^+, Ar^+ and Xe^+ ions so as to create a damaged layer, with the doses administered being higher than those previously reported. Modern Monte Carlo simulations (SRIM 2008) are utilised to provide an insight into the ion–graphite interactions, and the effects of varying ion penetration depths are considered when analysing the observed damage.

1. Introduction

It is well known that the irradiation of graphite can lead to a variety of changes to its mechanical and physical properties [1]. Such changes are of interest particularly to those in the nuclear industry where graphite has been widely used as a neutron moderator and is also a candidate for neutron moderation in some of the new Gen IV reactor designs [2]. High energy neutrons colliding with the carbon atoms as they undergo thermalisation generate a large number of atomic displacements such as interstitial/vacancy (Frenkel) pairs [3], affecting the microstructure of the graphite. Such processes are responsible for the breakdown of long-range order throughout the graphite lattice which, under prolonged irradiation, can tend to a more amorphous-like structure and consequently to a general weakening of the graphite brick [4].

Other concerns involve a build-up of potential energy known as Wigner energy [5] which can occur as a result of lattice strain caused through the generation of interstitial carbon atoms [6]. Despite many modern reactors operating at temperatures high enough to self-anneal any Wigner energy, the problem still remains for older, lower-temperature reactor cores, used particularly throughout the UK, which now require decommissioning.

Therefore, to improve the safety of the nuclear industry, it is important to understand the affects of neutron irradiation on the graphite moderator. A simple, effective and convenient method of doing this is to irradiate with ions, a technique employed regularly by those in the semi-conductor industry [7]. Ion bombardment leads to the same collision mechanisms and will also produce many Frenkel pairs within the graphite lattice; this allows research in this area to be pursued without the need for expensive hot-cell facilities [8].

To study the effects of ion irradiation on graphite, Raman spectroscopy has been used as it is known to be very effective at detecting the presence of defects, and can provide a quantitative measurement of the damage induced. Tuinstra and Koenig were the first to utilise Raman to study a graphite single crystal, where they observed a single large peak at 1575 cm^{-1} which they assigned to the E_{2g} mode of the infinite crystal, known as the *G* (graphite) band [9]. They also looked at other graphitic material, such as activated charcoal and carbon black and found that a new peak is present near 1355 cm^{-1}, known as the *D* (disorder) band, the intensity of which, when compared to that of the 1575 cm^{-1} band seemed to depend on the type of graphitic material studied. The increase in intensity was found to correspond to an increase in disordered carbon and a decrease in crystallite size; hence the band was attributed to a particle size effect and the authors related the relative intensity of the *D* band to the *G* band, the I_D/I_G ratio, to the inverse of the crystallite size through the following equation [10]:

$$\frac{I(D)}{I(G)} = \frac{4.4 \times 10^{-9}\ \mathrm{m}}{L_a} \tag{1}$$

Subsequently, many authors have used Raman spectroscopy to measure the effects of ion irradiation on graphite, with particular interest being shown by Japanese groups in the early 1990s. These researchers observed that as the ion-irradiation dose increased then so did the I_D/I_G ratio, up to a particular dose, after which the signal became less affected and eventually saturated; this observation was attributed to the production of vacancy clusters. In this paper we examine the effect of employing a higher ion energy of 5 keV; this is a small but significant increase, which along with a relatively high ion dose compared with previous studies, results in an increased I_D/I_G ratio. Computer simulation is also employed to study the ion–graphite interactions, with more accurate results being available than previously.

* Corresponding author. Tel.: +44 2920 874139; fax: +44 2920 874030.
E-mail addresses: alextheo250@hotmail.com (A. Theodosiou), carley@cardiff.ac.uk (A.F. Carley), taylorsh@cardiff.ac.uk (S.H. Taylor).

0022-3115/$ - see front matter © 2010 Elsevier B.V. All rights reserved.
doi:10.1016/j.jnucmat.2010.06.007

2. Material and methods

Highly-orientated pyrolytic graphite (HOPG) was supplied by SPI Supplies (http://www.2spi.com/). Samples ($5 \times 5 \times 1$ mm^3) were irradiated in a custom-built stainless steel UHV chamber (base pressure < 10^{-8} Pa) equipped with a Vacuum Generators AG2 cold-cathode ion gun, positioned with its axis normal to the sample. Samples were irradiated with increasing doses of inert gas ions He^+, Ne^+, Ar^+ and Xe^+ at room temperature, with doses not exceeding 5.0×10^{19} ions m^{-2}. Sample currents were measured with a multimeter connected to the target through an electronically isolated probe. The ion flux was approximately 5.0×10^{16} ions m^{-2} s^{-1} and Raman measurements were taken after irradiation for periods of 10, 20, 40, 80, 160 and 320 s.

Raman measurements were carried out using a LabRam HR confocal microscope from HORIBA Jobin Yvon Ltd. Incident illumination of wavelength 514.5 nm was provided by a cw argon-ion laser and any annealing effects were considered negligible. The spectrometer was equipped with a 50× long working distance objective lens with a numerical aperture of 0.55 and a working distance of 8.1 mm, producing a spot size of 1.4 μm. A 10× condenser lens with a focal length of 300 mm was used to focus the laser onto the objective lens. A 1024 pixel CCD peltier cooled detector was used to detect the scattered radiation. The resultant Raman spectra were analysed using the Labspec 5.0 software and accurate peak intensities were obtained through numerical decomposition by assuming a Lorentzian line shape for all peaks.

3. Theory/calculation

The interaction of ions with matter is a complex field and has been studied intensely by many authors [11–14]. An ion, travelling with sufficient energy, may transfer a proportion of this energy to a host atom causing the atom to be displaced from its lattice site. This atom may then go onto do the same and remove other host atoms, leading to a collision cascade. Such mechanisms are responsible for atomic displacement and hence the production of damage within ion-irradiated materials. The extent of these collision cascades and thus the amount of damage generated is dependant primarily on ion energy and the mass of the incident ion relative to the target atom.

It is known that as ion energy increases, then the depth at which the damage occurs also increases, since the ions can penetrate more deeply into the target material before coming to rest. The ion mass also is important, and for a particular kinetic energy, lighter ions will travel further into the target as they have relatively small collision cross-sections and will collide with the host infrequently, compared to a larger ion.

The Stopping and Range of Ions in Matter (SRIM 2008)[1] is a software code which uses Monte Carlo techniques to effectively predict the behaviour of ions in matter [15]. This code is an updated version of the TRIM85 and TRIM89 codes, used extensively in this field throughout the 1990s. The damage profile within a target caused by ion bombardment is known to be approximated by a Gaussian function [16]. The SRIM 2008 code can calculate this for many ion/solid interactions and results for the irradiation of graphite by 5 keV He^+, Ne^+, Ar^+ and Xe^+ ions are presented in Table 1.

Fig. 1 is a simulation of the distribution of the ions, initially travelling with 5 keV energy, as they enter the graphite matrix. The effect of ion mass is clearly observed, with He^+ ions spreading themselves across a relatively large range throughout the target whereas the much larger Xe^+ ions implant over a very short range, with the vast majority being located at approximately 7 nm.

[1] www.srim.org

Table 1
Parameters of the damage profile approximated by a Gaussian function for the irradiation of graphite by 5 keV ions. χ_0 is the mean implantation depth, σ is the standard deviation and P is the whole range of energy distribution, i.e., the range over which the ions deposit all their kinetic energy.

Ion	Ion mass (amu)	χ_0 (nm)	σ (nm)	P (nm)	Vacancies/ion
He^+	4.00	23	29	88	29
Ne^+	19.99	3	6.25	22	60
Ar^+	39.96	1.5	4	12	63
Xe^+	131.9	0.7	3	9	74

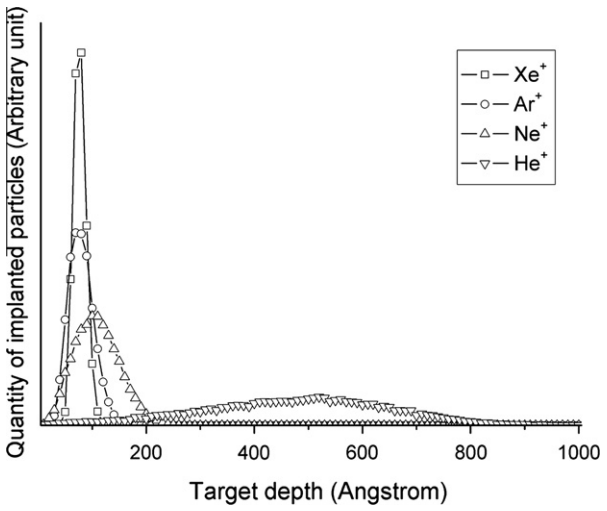

Fig. 1. The implantation profiles of 5 keV He^+, Ne^+, Ar^+ and Xe^+ ions in graphite modelled by the SRIM 2008 Monte Carlo program.

The difference in ion mass and the consequent difference in their implantation profiles results directly in a difference in the amount and rate of damage caused. Table 1 indicates that larger ions will create more atomic displacements leading to more vacant sites, which is as expected due to the larger collision cross-sections. Lighter ions will travel much further distances between ion interactions since electronic stopping predominates, resulting in a much lower amount of energy loss per collision and thus significantly lower vacancy production.

4. Results

Fig. 2a–d shows the time-resolved series of Raman spectra obtained for the room temperature irradiation of HOPG with 5 keV He^+, Ne^+, Ar^+ and Xe^+ ions. The virgin spectra are shown at the bottom of each graph and clearly consist of only one band, the well known graphite band (G-band) at 1580 cm^{-1}. Each spectrum in a sequence is measured after twice the total irradiation time (dose) of the previous one.

Consistent features were observed for each of the ions studied, with trends agreeing with previously reported results [17–19]. The observed bands arise from the activation of Raman active vibrational modes, the details of which can be found elsewhere [20–22]. The emergence of the disorder induced D band at ca. 1350 cm^{-1} is the prominent feature, which steadily increases in intensity with increasing fluence; simultaneously, the intensity of the G band slowly decreases resulting in an increased I_D/I_G ratio.

Other notable features include an increase in the line-width of the D band and a pronounced increase in intensity in the region between the D and G bands, in the range 1400–1580 cm^{-1} which is particularly prominent at higher doses. The extent of the broadening seems to be more significant for the He^+ irradiated samples, and is likely to be due to the smaller ion mass [23].

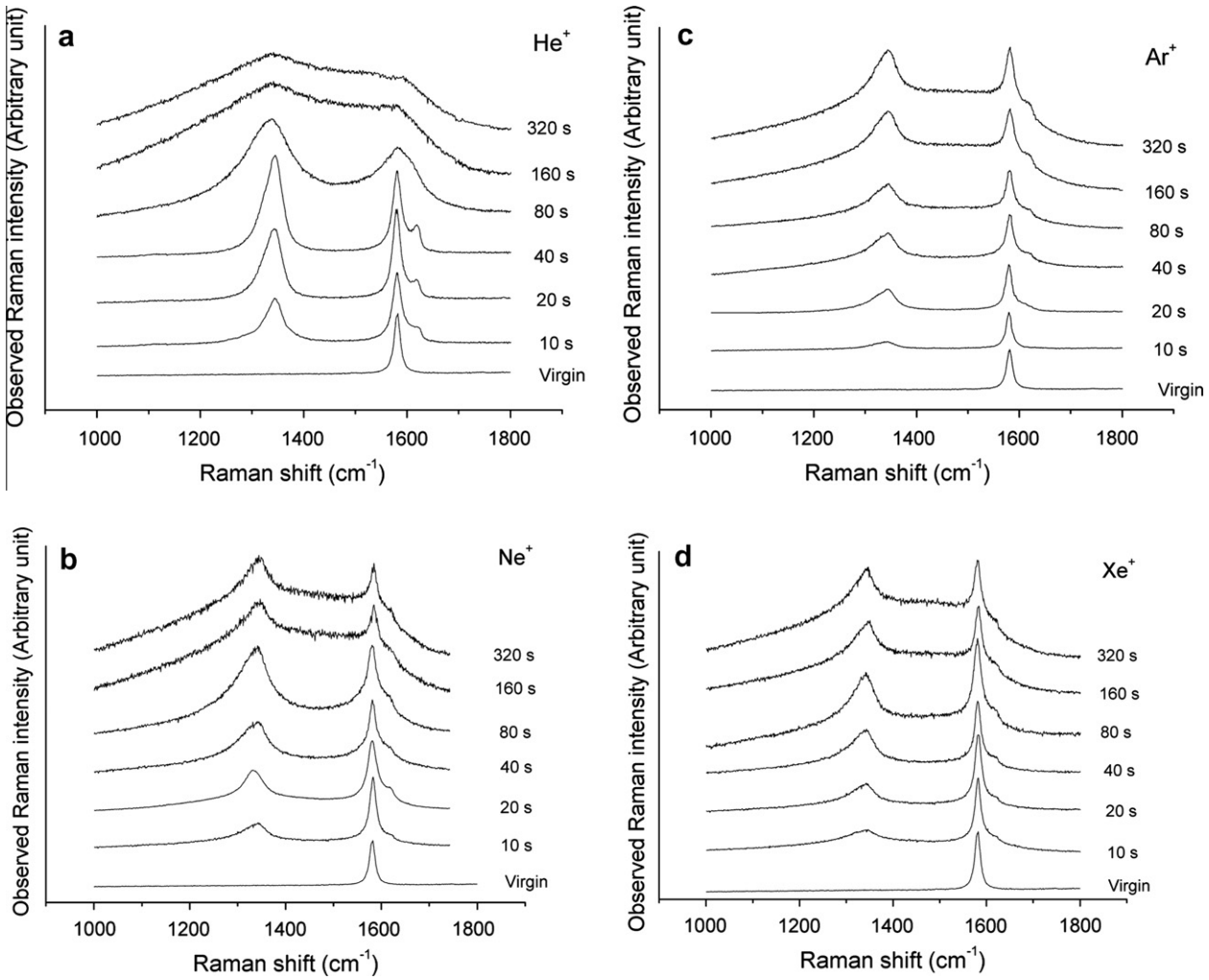

Fig. 2. Time-resolved Raman spectra obtained after 5 keV ion irradiation of HOPG with (a) He^+ (top-left), (b) Ne^+ (top-right), (c) Ar^+ (bottom-left) and (d) Xe^+ (bottom-right) at a flux of 5.0×10^{16} ions m^{-2} s^{-1}. Features of interest include the *D* band (ca. 1355 cm^{-1}), the *G* band (ca. 1580 cm^{-1}) and the *D′* band (ca. 1620 cm^{-1}) as shown in the bottom left panel.

The so-called *D′* peak centred at 1620 cm^{-1} becomes apparent after 10 s irradiation, and increases in intensity before becoming a shoulder to the *G* band and eventually becoming almost indistinguishable from it at higher fluences. In the case of He^+ bombardment the *D′* peak seems to be more prominent up to an irradiation time of 80 s, where again it merges with the *G* band.

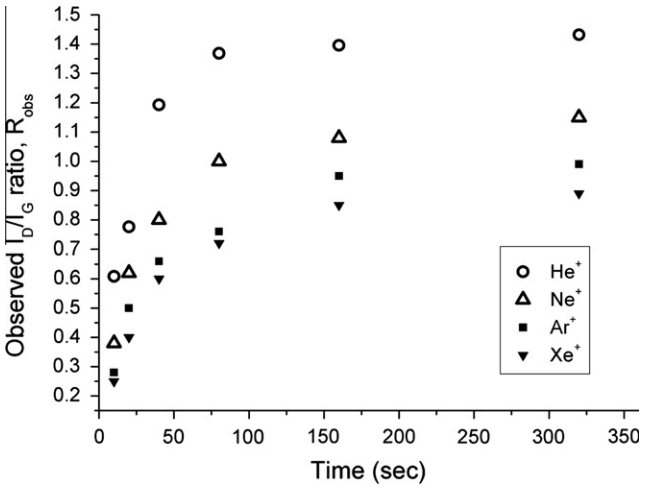

Fig. 3. Dependence of R_{obs}, the observed ratio of the intensities of the Raman disorder and graphite bands, on the ion irradiation time, for He^+, Ne^+, Ar^+ and Xe^+ ions.

Fig. 3 shows the observed I_D/I_G ratios, R_{obs}, for each of the ions studied, plotted against the irradiation time. R_{obs} initially increases proportionally with respect to time before deviating and reaching a plateau. Since the I_D/I_G ratio is known to be inversely proportional to the crystallite size, L_a [9] it can be a useful method of measuring and monitoring the build-up of damage within a graphite sample. The differences observed in Fig. 3 agree with the Monte Carlo estimations of the implantation depth (cf. Fig 1).

5. Discussion

Since the depth which the Raman laser samples within graphite (known as the optical skin depth) is ca. 40 nm [18,19], a value larger than the penetration depth of the ions in this study (cf. Table 1), we can deduce that the observed peak intensity ratio, R_{obs}, consists of a superposition of information taken from both damaged and underlying undamaged volumes of the sample, and hence can be a misleading representation of the true ion effects. The intensity ratio taken from the damaged layers only, R_0, provides a more accurate assessment of ion effects and can be readily calculated

from Eq. (2), which is a corrected version of that reported in the literature [19,24]:

$$R_{obs} = \frac{8R_0 P\pi m}{\lambda} \int_0^\infty F(x)\exp(-8\pi m x/\lambda)dx \quad (2)$$

where P is the whole range of energy deposition (cf. Table 1), m is the optical parameter (0.9 for carbon material [19]), λ is the wavelength of the exciting light, x is the depth and $F(x)$ is the depth profile of the damaged layer, normalised to unity.

Essentially Eq. (2) provides a method of estimating the actual extent of damage occurring upon ion irradiation, for situations where the ions do not enter the target material further than the optical skin depth. Fig. 3 displays the data obtained directly from the Raman experiment; however it must be adjusted in order to show the actual ion affects. From Eq. (2) the intensity ratios in the damaged region only are calculated to be 1, 1.5, 2, and 3 times the magnitude of R_{obs} for He^+, Ne^+, Ar^+ and Xe^+ ions respectively. From Fig. 1 we can see that the 1:1 R_0:R_{obs} ratio observed for He^+ is expected, since 5 keV He^+ ions lose their energy around the optical skin depth anyway and so no adjustments are needed, however for the other ions studied they do not reach the optical skin depth and therefore Eq. (2) must be used. In Fig. 4 the plot in Fig. 3 is corrected to the Raman intensity from the damaged region only, which simply involves multiplying the values by the factor stated above, calculated through Eq. (2). These values are lower than those obtained for the same radiation at 3 keV [19,24] and can be explained by the increase in ion penetration depth, which at 5 keV is much closer to the optical skin depth; therefore a lower percentage of the Raman signal is from the undamaged region.

For each of the ions studied an increase in $R_0 = I_D/I_G$ is observed, up to an irradiation time of approximately 80 s (fluence = 4.0×10^{18} ions m^{-2}) after which it starts to plateau indicating the beginning of damage saturation. As expected an increase in ion mass leads to an increase in R_0 since heavier, larger ions can interact with more of the host atoms, causing significant damage [18]. Previously Nakamura and Kitijama [16] have explained the increase in the I_D/I_G ratio on the ion-induced reduction in the phonon correlation length which, can be explained by the creation of defects that can interact and interrupt the phonon path. For lower fluences this is responsible for the initial proportional rise of R_0 with respect to time.

Although the extent of the damage appears to saturate, from Fig. 2 we can see that this is not the case – in the case of He^+ for example, there are considerable differences in the spectra obtained between 80 s and 320 s irradiation time, despite a very similar I_D/I_G ratio. Therefore, as observed previously, the I_D/I_G ratio is not valid at higher fluencies to describe the ion-induced damage; as a linear trend is no longer observed. This has been attributed to the breakdown of the relation between R_0 and the phonon correlation length at higher fluence [25], proposed to be due to a kinetic process of point defects, indicating a saturation of vacancy concentration at higher irradiation dose [26].

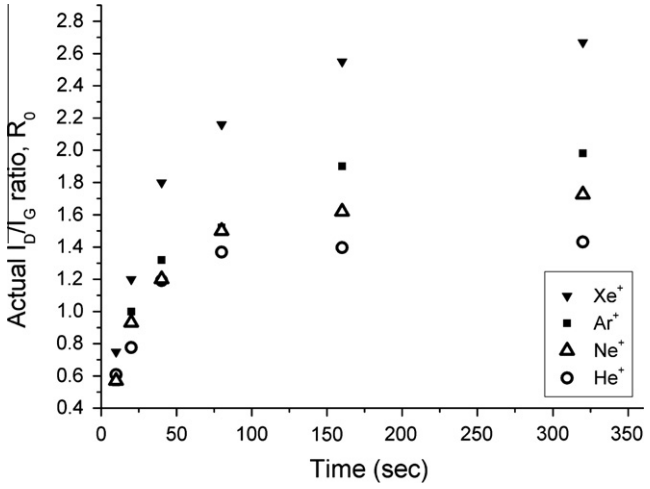

Fig. 4. Dependence of R_0 (calculated from Eq. (1)) on the ion irradiation time, for He^+, Ne^+, Ar^+ and Xe^+ ions.

The saturation of R_0 has been explained by the creation of di-vacancies and vacancy clusters which are expected to have a negligible effect on the phonon correlation length, since a di-vacancy, for example, would form by two adjacent carbon atoms being removed and hence the mean distance between defects would not be changed significantly [27]. The probability of the generation of vacancy clusters has been enhanced in this case due to the relatively high ion doses administered, leading to a more pronounced overlap of collision cascades, as modelled through SRIM 2008.

Therefore the difference observed in the spectra, after an irradiation time of 80 s, must be due to some other factor. It is likely that the broad increase in the spectra around 1500 cm^{-1} and the general broadening of the spectra are a result of significant lattice disruption and a considerable breakdown of long-range order. Niwase has explained the observed broadening to be due to the life time broadening of phonons originating in the lattice distortion around the dislocation dipole, which grows as a result of prolonged irradiation [28]. It is expected that after a certain higher irradiation dose the spectra observed becomes completely saturated, with the area between the two peaks increasing such that a single, very broad feature is observed throughout the entire first order region, suggesting considerable loss of crystallinity and the development of amorphous-like structure. Such Raman spectra have been observed recently in graphite exposed to edge plasma in the TEXTOR tokamak [29].

6. Conclusions

The effect of ion energy has been shown to be crucial to the Raman data observed, due to its direct affect on the ion penetration depth. This effect has proved to be significant even for a relatively small energy increase from 3 keV (published previously) to 5 keV. It is also observed that although the I_D/I_G ratio is an effective measure of damage; after a critical fluence, other aspects of the spectra must also be considered. After a fluence of 4.0×10^{18} m^2 s a disorder-induced broader band emerges at ca. 1500 cm^{-1} which again starts to increase in intensity with increasing dose. Its origin is likely due to complex defect formation, and a severe breakdown of crystallinity; however further investigation is required on the exact nature of the defects produced and the origin of this Raman band.

Acknowledgements

The authors would like to thank Prof. Barry Marsden, Dr. Abbie Jones and Michael Lasithioakis from the Manchester Nuclear Graphite Research Group for support and encouragement. This work was carried out as part of the TSEC programme KNOO and as such we are grateful to the EPSRC for funding under grant EP/C549465/1. We wish to thank Dr. Colin Rhodes (NDA) in particular for his suggestions which inspired this research.

References

[1] B.T. Kelly, Carbon 20 (1982) 3.
[2] L.K. Mansur, A.F. Rowcliffe, R.K. Nanstad, S.J. Zinkle, W.R. Corwin, R.E. Stoller, J. Nucl. Mater. 166 (2004) 329.
[3] K. Niwase, Phys. Rev. B 22 (1995) 52.

[4] D.R. De Halas, Theory of radiation effects in graphite, in: R.E. Nightingale (Ed.), Nuclear Graphite, Academic Press, New York and London, 1962.
[5] E.P. Wigner, CP-387, 1942.
[6] R.H. Telling, C.P. Ewels, A.A. El-Barbary, M.I. Heggie, Nature Mater. 2 (2003) 333.
[7] J.W. Mayer, L. Eriksson, J.A. Davies, Ion Implantation in Semiconductors, Academic Press, 1970.
[8] C. Abromeit, J. Nucl. Mater. 216 (1994) 78.
[9] F. Tuinstra, J. Koenig, J. Chem. Phys. 53 (1970) 1126.
[10] K.G. Nakamura, M. Kitakima, Appl. Phys. Lett. 59 (1991) 1550.
[11] M. Nastasi, J.W. Mayer, J.K. Hirvone, Ion–Solid Interactions: Fundamentals and Applications, Cambridge University Press, 1996.
[12] G.H. Kinchin, R.S. Pease, Rep. Prog. Phys. 18 (1955) 1.
[13] E.J. Parillis, L.M. Kishinevsky, B.E. Baklitsky, Atomic Collisions on Solid Surfaces, North Holland Elsevier, 1993.
[14] R.S. Averback, J. Nucl. Mater. 108–109 (1982) 33.
[15] J.F. Ziegler, J.P. Biersack, M.D. Ziegler, The Stopping and Range of Ions in Matter, SRIM Co., USA, 2008.
[16] K. Nakamura, M. Kitajima, Phys. Rev. B 45 (1992) 78.
[17] K.G. Nakamura, M. Kitakima, J. Nucl. Mater. 187 (1992) 294.
[18] K.G. Nakamura, M. Kitakima, Phys. Rev. B 45 (1992) 5672.
[19] K.G. Nakamura, M. Kitakima, Surf. Sci. 283 (1993) 255.
[20] S. Reich, C. Thomsen, Philos. Trans. Roy. Soc. Lond. A 362 (2004) 2271.
[21] A.C. Ferrari, J. Robertson, Phys. Rev. B 61 (1999) 14095.
[22] R.J. Nemanich, S.A. Solin, Phys. Rev. B 20 (1979) 392.
[23] K.G. Nakamura, M. Fujitsuka, M. Kitajima, Phys. Rev. B 41 (1990) 12260.
[24] E. Asari, I. Kamioka, K.G. Nakamura, T. Kawabe, W.A. Lewis, M. Kitajima, Phys. Rev. B 49 (1994) 1011.
[25] D.S. Knight, W.B. White, J. Mater. Res. 4 (1989) 385.
[26] K. Niwase, Philos. Mag. Lett. 82 (2002) 401.
[27] E. Asari, Carbon 38 (2000) 1857.
[28] K. Niwase, Mater. Sci. Eng. A 400–401 (2005) 101.
[29] T. Hirai, J. Compan, K. Niwase, J. Linke, J. Nucl. Mater. 373 (2008) 119.